BBA - Bioenergetics 1860 (2019) 181–188

Contents lists available at ScienceDirect

BBA - Bioenergetics

journal homepage: www.elsevier.com/locate/bbabio

Residue 249 in subunit beta regulates ADP inhibition and its phosphate modulation in *Escherichia coli* ATP synthase

Anna S. Lapashina[a,b], Anastasia S. Prikhodko[a], Tatiana E. Shugaeva[b], Boris A. Feniouk[a,b,*]

[a] Belozersky Institute of Physico-Chemical Biology, Lomonosov Moscow State University, 119991 Moscow, Russia
[b] Faculty of Bioengineering and Bioinformatics, Lomonosov Moscow State University, 119991 Moscow, Russia

ARTICLE INFO

Keywords:
ATP synthase
Regulation
ADP-inhibition
Phosphate
Escherichia coli
Sulfite

ABSTRACT

ATPase activity of proton-translocating F_OF_1-ATP synthase (F-type ATPase or F-ATPase) is suppressed in the absence of protonmotive force by several regulatory mechanisms. The most conservative of these mechanisms found in all enzymes studied so far is allosteric inhibition of ATP hydrolysis by MgADP (ADP-inhibition). When MgADP is bound without phosphate in the catalytic site, the enzyme lapses into an inactive state with MgADP trapped.

In chloroplasts and mitochondria, as well as in most bacteria, phosphate prevents MgADP inhibition. However, in *Escherichia coli* ATP synthase ADP-inhibition is relatively weak and phosphate does not prevent it but seems to enhance it.

We found that a single amino acid residue in subunit β is responsible for these features of *E. coli* enzyme. Mutation βL249Q significantly enhanced ADP-inhibition in *E. coli* ATP synthase, increased the extent of ATP hydrolysis stimulation by sulfite, and rendered the ADP-inhibition sensitive to phosphate in the same manner as observed in F_OF_1 from mitochondria, chloroplasts, and most aerobic\photosynthetic bacteria.

1. Introduction

F_OF_1 ATP synthase is a membrane multisubunit enzyme that catalyzes synthesis of ATP from ADP and inorganic phosphate (P_i). The enzyme is found in bacterial plasma membrane, in the inner mitochondrial membrane and in thylakoid membrane in chloroplasts. The hydrophilic catalytic F_1-portion of the enzyme protrudes from the membrane and bears nucleotide-binding sites. The hydrophobic F_O-portion is embedded in the membrane and is responsible for proton transport. Subunit composition of *Escherichia coli* catalytic portion F_1 is $\alpha_3\beta_3\gamma_1\delta_1\varepsilon_1$; the membrane part F_O consists of three types of subunits in stoichiometry $a_1b_2c_{10}$ [1,2]. ATP synthesis catalyzed by F_1 is coupled to H^+-transport through F_O via a rotary mechanism (see [3–5] for recent reviews). Driven by protonmotive force (*pmf*), protons pass at the interface of subunit *a* and the c_{10} oligomeric ring and induce the rotation of the ring relative to the ab_2-complex. The latter is bound to $\alpha_3\beta_3\delta_1$-complex, while subunits γ and ε are bound to the *c*-ring and rotate together with it relative to the $\alpha_3\beta_3\delta_1$-complex. Rotation of subunit γ inside the $\alpha_3\beta_3$ hexamer induces sequential conformational changes that result in ADP and P_i binding, ATP synthesis and release. Upon decrease or dissipation of *pmf* the reaction is reversed. ATP hydrolysis induces conformational changes in $\alpha_3\beta_3$ that drive the rotation of $\gamma\varepsilon ac_{10}$-complex. The rotation of the c_{10}-ring relative to subunit *a* results in transmembrane proton transport and in generation of *pmf*.

The ATPase activity of F_OF_1 might be important under conditions when the activity of the primary *pmf*-generating enzymes drops. Dark time for photosynthetic bacteria and lack of oxygen or of nutrients for aerobic bacteria are examples of such conditions. Maintaining *pmf* at the expense of ATP hydrolysis is necessary in such situation to support flagella rotation and motility, transmembrane transport of ions and of organic molecules, etc. However, when the intracellular ATP concentration significantly decreases or when the membrane permeability to protons is increased, e.g. by uncouplers or toxins, ATP hydrolysis by F_OF_1 might exhaust the ATP pool and poses a threat to the cell. Thus, it is not surprising that the ATPase activity of F_OF_1 is down-regulated by several mechanisms [6–9].

Non-competitive inhibition of ATP hydrolysis by MgADP is probably the most conservative of these mechanisms and is found in all F-ATPases studied so far (see [10] for a recent review). If the membrane is de-energized and MgADP is bound in the catalytic site without P_i, the enzyme may occasionally undergo a conformational transition into an inactive state with ADP trapped in the catalytic site. In mitochondrial, chloroplastic and most bacterial ATP synthases, P_i counteracts this transition. Re-activation of the inhibited F_OF_1 requires membrane

* Corresponding author at: Faculty of Bioengineering and Bioinformatics, Lomonosov Moscow State University, Leninskie Gory 1-73, 119991 Moscow, Russia.
E-mail address: feniouk@fbb.msu.ru (B.A. Feniouk).

https://doi.org/10.1016/j.bbabio.2018.12.003
Received 28 September 2018; Received in revised form 6 December 2018; Accepted 7 December 2018
Available online 07 December 2018
0005-2728/

energization: rotation of subunit γ driven by high *pmf* forces subunit β with the inhibitory ADP locked in the catalytic site into open state, ADP is released, and the enzyme re-gains activity. On the other hand, moderate membrane energization also counteracts ADP-inhibition by increasing the affinity of catalytic sites to phosphate, thereby lowering the probability of ADP being bound in the catalytic site without P_i.

However, the pattern of ADP-inhibition in *E. coli* F_OF_1 (EF_OF_1) seems to be different from that described above. First, *E. coli* enzyme is less vulnerable to ADP-inhibition than other ATP synthases studied so far. Pioneer attempts to describe the inhibitory effect of MgADP on EF_1 did not give any result [11], since the inhibitory subunit ε camouflaged the weak inhibition of ATP hydrolysis by MgADP ([12], for a detailed review see [10]). Second, the ADP-inhibition of EF_OF_1 is not prevented, but rather enhanced by P_i [13,14]. In this study, we had compared the wild type and βL249Q EF_1 and EF_OF_1 complexes, and had revealed that the βL249Q mutation enhanced ADP-inhibition and reversed the inhibitory effect of P_i. In mitochondrial, chloroplastic and most bacterial enzymes the residue in the corresponding position is Gln, while in many gammaproteobacteria (including *E. coli*) and betaproteobacteria it is Leu. We have demonstrated earlier that Gln to Leu substitution at this position diminishes ADP-inhibition in F_OF_1 from thermophilic *Bacillus* sp. PS3 [15]. It seems that the mutation switched the mode of ADP-inhibition from '*E. coli* type' to the variant described for F_OF_1 from *Bacillus* sp. PS3, *Rhodobacter capsulatus*, *Paracoccus denitrificans*, mitochondria and chloroplasts.

2. Materials and methods

2.1. E. coli strains, cultivation procedures, and mutagenesis

Plasmid pFV2 encoding a cysteine-less *E. coli* ATP synthase with a 6xHis-tag at the amino terminus of the β subunit was used for both site-directed mutagenesis and protein expression [16]. In this study, the enzyme obtained from this plasmid without additional mutations is referred to as 'wild type' enzyme. The L249Q mutation in β subunit was introduced into pFV2 sequence using polymerase chain reaction with mutagenic primer 5′-GCTGTTCGTTGACAACATCTATCGTTACACC**CAG** GCCGGTAC**C**GAAGTATCCGCACTGCTGGGCCGTATGC-3′ and wild type pFV2 as a template. Briefly, two primers, one of which introduced the mutation, were used to synthesize a ~250 bp oligonucleotide (megaprimer) carrying the mutation and the nearest endonuclease restriction site unique for pFV2. Then, a third primer was used to extend the mutation-containing fragment to flank the mutation with another unique restriction site. The fragment was cloned into pBluescript II SK(−) cloning vector, sequenced and transferred into pFV2. All clonings were performed in *E. coli* strain XL-1 Blue. Mutant or wild type variants of pFV2 were expressed in *E. coli* strain BW25113 (ΔatpB-atpC), in which most of ATP synthase coding operon was replaced with kanamycin resistance cassette according to [17].

2.2. Inverted membrane vesicles preparation

E. coli cells carrying wild type or mutant pFV2 were grown aerobically for 7–8 h at 37 °C with shaking in 3 ml LB medium containing 100 μg/ml ampicillin (Amp), then 1 ml of the culture was inoculated into 600 ml of fresh LB + Amp in 2 l Erlenmeyer flask to grow overnight at the same conditions. For one preparation, total culture volume was 3 l (5 flasks), typically giving a yield of 15–20 g of *E. coli* cells (wet weight). Cells were harvested by centrifugation (10,000*g*, 10 min), washed with membrane preparation buffer (10 mM HEPES-NaOH, pH 7.5, 5 mM $MgCl_2$, 10% glycerol), resuspended in 25–30 ml of the same buffer and disrupted by two subsequent French press passages at 1000 p.s.i. Unbroken cells were collected by centrifugation at 13,700*g* for 30 min and discarded. The supernatant fraction was centrifuged at 390,000*g* for 1 h to collect membrane vesicles, which were then resuspended in 25 ml of preparation buffer and centrifuged once more. Finally, membrane vesicles were resuspended in 1–1.5 ml of preparation buffer. Starting from cell disruption, all manipulations were performed at 4 °C or on ice. For ATP synthase activity measurements, membrane vesicles suspension was frozen in 50 μl aliquots in liquid nitrogen and stored at −80 °C. Protein concentration in the suspension was determined with Pierce BCA Protein Assay Kit by Thermo Fisher Scientific, using BSA solutions as a reference. Typical protein concentration in the membrane vesicles suspension was 20–80 mg/ml.

2.3. Enzyme purification

In this work, we slightly modified the method of His-tagged EF_OF_1 purification by Ishmukhametov et al. [16]. All manipulations were performed at 4 °C unless specified otherwise. Membrane vesicles obtained from 15 to 20 g of *E. coli* cells were resuspended in 10 ml of extraction buffer (50 mM Tris-HCl, pH 7.5, 100 mM KCl, 250 mM sucrose, 40 mM ε-aminocaproic acid, 15 mM *p*-amino-benzamidine, 5 mM $MgCl_2$, 0.1 mM EDTA, 0.2 mM DTT, 0.8% phosphatidylcholine, 1.5% octyl glucoside, 0.5% sodium deoxycholate, 0.5% sodium cholate, 2.5% glycerol) supplemented with 30 mM imidazole and kept on ice for 90 min on a shaking platform (70–90 rpm). The extract was centrifuged at 390,000*g* for 1 h. The supernatant was applied to a Ni-NTA column containing 2 ml of resin and equilibrated with extraction buffer supplemented with 30 mM imidazole. The resin was then washed with 20 ml of the same buffer to remove contaminants. After that, EF_OF_1 was eluted with 3 ml of extraction buffer supplemented with 150 mM imidazole. To wash off imidazole, the eluate was applied to a PD-10 Desalting column (GE Healthcare) equilibrated with extraction buffer. The resulting EF_OF_1 was concentrated with Amicon Ultra-15 Centrifugal Philter Unit (Ultracel-100K membrane, Merck) to 10–20 mg/ml, aliquoted, and kept at −80 °C until use. The protein concentration in EF_OF_1 samples was estimated by Bradford assay; the subunit composition of EF_OF_1 was verified with SDS-PAGE (see the Supplementary material). Typically, total EF_OF_1 yield from 15 to 20 g of *E. coli* cells was 3–5 mg.

EF_1 was purified by chloroform extraction and subsequent Ni-NTA chromatography. Inverted membranes were resuspended in 3 ml membrane preparation buffer with 2 mM ATP and added to 6 ml chloroform (neutralized with 100 mM phosphate buffer, pH 8). The mixture was shaken for 30 s and centrifuged at 4000*g*, 4 °C for 5 min. Aqueous upper phase was then centrifuged at 390,000*g*, 4 °C for 45 min. The supernatant was applied on a 1 ml Ni-NTA agarose column equilibrated with 3 volumes of buffer containing 50 mM HEPES-KOH, pH 8, 100 mM KCl, 5 mM $MgCl_2$, 2.5% glycerol, and 50 mM imidazole. The column was washed with 30 ml of the same buffer, and then the protein was eluted by the same buffer but with 200 mM imidazole. Fractions containing protein were pooled, concentrated on Amicon Ultracel-100K concentrator and passed through a Nap10 gel filtration column equilibrated with 10 mM HEPES-NaOH, pH 7.5, 5 mM $MgCl_2$, 10% glycerol. After buffer exchange the sample was concentrated on Amicon Ultracel-100K concentrator to 6–10 mg protein per ml, aliquoted and kept at −80 °C until use. The subunit composition of EF_1 was verified with SDS-PAGE (see the Supplementary material).

2.4. EF_OF_1 reconstitution into liposomes

Phosphatidylcholine liposomes were prepared by sonication in buffer L containing 10 mM HEPES, pH 7.5, 100 mM NaCl, 2.5 mM $MgCl_2$, 10% (w/v) glycerol. Lipid (L-α-phosphatidylcholine from soybean, Sigma, P5638) concentration in the suspension of liposomes was 20 mg/ml. Reconstitution of EF_OF_1 was carried out at room temperature. The liposomes suspension diluted with buffer L to 8 mg/ml was mixed with Triton X-100 (to 0.8%) and EF_OF_1 (to 0.16 mg/ml) and mildly shaken for 1 h. To wash off the detergent, Bio-Beads SM-2 resin (Bio-Rad Laboratories) presoaked in buffer L was added to the suspension to 320 mg/ml. After 2.5 h shaking, the proteoliposomes

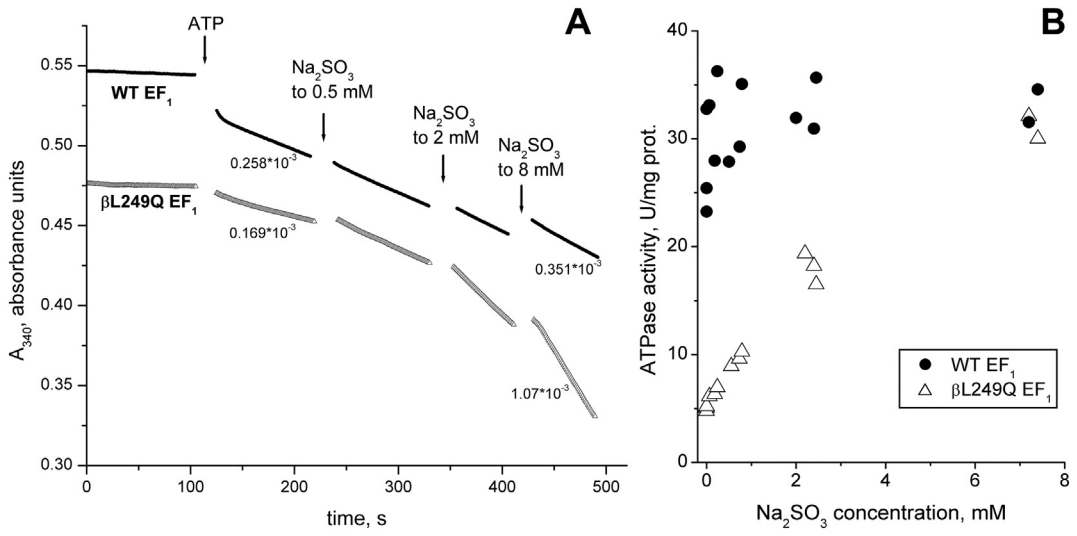

Fig. 1. ATPase activity of the wild type and of βL249Q EF_1 measured by NADH assay (see Materials and methods). A - raw traces. The reaction was initiated by addition of ATP to 1 mM, and then sulfite was added to concentrations indicated. Rates at 0 and 8 mM sulfite are given below the traces. Concentrations of WT and mutant EF_1 were 0.1 μg/ml and 0.3 μg/ml, respectively; B - dependence of the ATPase activity on sulfite concentration. 1 U corresponds to 1 μmol ATP hydrolyzed per 1 min.

suspension was collected on a filtered column. Samples were stored for several days at 4 °C; the loss of ATPase activity during storage did not exceed 10%.

2.5. Enzymatic assays

2.5.1. Phenol red assay

ATP hydrolysis activity was measured by following proton release using the pH indicator phenol red in buffer containing 2 mM HEPES-NaOH, pH 8.0, 100 mM KCl, 1 or 2.5 mM $MgCl_2$, 30 μM phenol red. The indicator response was registered as absorbance change at 560 nm corrected by absorbance at isosbestic point (477 nm) and calibrated in each sample by NaOH additions to 100 μM. Hydrolysis was started by addition of ATP or ATP/ADP mixture (pH adjusted to 8.0); total nucleotide concentration in each sample was 1 mM. When indicated, samples also contained 3 mM potassium phosphate, 5 mM sulfite, or valinomycin + nigericin, 500 nM each. Measurements were performed at 37 °C on Aminco DW-2000 spectrophotometer or on CLARIOstar (BMG Labtech) microplate reader.

2.5.2. NADH assay

ATPase activities were also measured in ADP scavenging system, when the hydrolysis of ADP was monitored optically at 340 nm via NADH oxidation enzymatically coupled with rephosphorylation of ADP produced by EF_OF_1. The reaction medium contained 50 mM HEPES-NaOH, pH 8.0, 100 mM KCl, 1 mM $MgCl_2$, 2.5 mM phosphoenolpyruvate, 80–125 μM NADH, pyruvate kinase and lactate dehydrogenase (40 units/ml each). Hydrolysis was started by addition of ATP to 1 mM. If specified, sulfite or valinomycin + nigericin (to 500 nM each) were added. Measurements were performed at 37 °C on Aminco DW-2000 spectrophotometer or on CLARIOstar (BMG Labtech) microplate reader.

2.5.3. ATP synthesis assay

The synthesis of ATP was measured by luciferin/luciferase assay (Roche ATP Bioluminescence CLS II kit) in Horiba Fluoromax-3 fluorimeter with excitation lamp switched off and emission set to 560 nm. The sample contained 900 μl of ATP synthesis buffer (20 mM HEPES-NaOH, pH 8.0, 100 mM potassium acetate, 10 mM potassium phosphate, 5 mM magnesium acetate, 75 μM ADP, 2 μM adenylate kinase inhibitor Ap5A) and 100 μl of luciferase reagent. In each sample, luciferase response was calibrated by three subsequent ATP additions to 100 nM. Sodium succinate was added to 4 mM to generate *pmf*. After ~1 min of ATP synthesis, *pmf* was dissipated by uncoupler addition (valinomycin + nigericin to 500 nM each). Measurements were performed at room temperature.

2.5.4. ACMA assay

ATP-driven proton pumping was detected by monitoring 9-amino-6-chloro-2-methoxyacridine (ACMA) fluorescence, which quenches when a pH gradient forms across the membrane. The ACMA buffer contained 10 mM HEPES-NaOH, pH 7.5, 100 mM KCl, 5 mM $MgCl_2$, 0.3 μg/ml ACMA. ACMA fluorescence was registered at 410 nm excitation and 480 nm emission in Horiba Fluoromax-3 fluorimeter. The pumping of protons was started by addition of ATP to 500 μM and later pH gradient was dissipated by addition of valinomycin + nigericin, each to 500 nM.

3. Results

3.1. ATPase activity of βL249Q mutant is reduced due to enhanced ADP-inhibition

We measured the ATPase activity of βL249Q mutant EF_1 with NADH assay under conditions when ADP produced as a product of ATP hydrolysis was removed by ATP-regenerating system. Noteworthy, under these conditions ADP-inhibition can still be present due to ADP being produced in the catalytic site as a result of ATP hydrolysis. The activity of the mutant enzyme was significantly lower than that of the wild type EF_1 (4.9 ± 0.3 versus 28.7 ± 4.6 U/mg protein; Fig. 1B). To clarify if the impaired activity was due to a stronger ADP-inhibition, we measured ATP hydrolysis in the presence of sulfite, which is known to relieve the inhibition [18–21]. As can be seen in Fig. 1, addition of sulfite up to 8 mM had no significant effect on the ATPase activity of the wild type EF_1. However, the mutant βL249Q EF_1 was markedly stimulated by sulfite. At 8 mM sulfite, the ATPase activity of the mutant EF_1 was approximately equal to that of the wild type enzyme (Fig. 1B). It should be noted that the concentrations of EF_1 in the samples (0.1 μg/ml, or ~0.26 nM for the wild type, and 0.3 μg/ml, or ~0.78 nM for the mutant) were below the K_D for subunit ε binding to EF_1 (3–10 nM [22–24]). Under such conditions, subunit ε was expected to dissociate from EF_1, and the observed effects of sulfite were likely unrelated to the inhibitory effects of subunit ε.

Similar results were obtained for the whole EF_OF_1. Measurements of

Table 1
ATPase activity of inverted *E. coli* membranes and of proteoliposomes with wild type and βL249Q mutant EF_OF_1 measured by phenol red assay as described in Materials and methods.

Hydrolysis of 1 mM ATP measured by phenol red assay, 37 °C, U/mg protein ± SD		
	Wild type	βL249Q
Inverted membrane vesicles, coupled	5,15 ± 0,88	0,59 ± 0,12
Inverted membrane vesicles, uncoupled	7,08 ± 1,32	0,74 ± 0,14
Proteoliposomes, coupled	9,87 ± 1,38	0,84 ± 0,13
Proteoliposomes, uncoupled	20,9 ± 2,67	1,32 ± 0,24

the ATP hydrolysis rate in inverted *E. coli* membranes and in proteoliposomes with purified EF_OF_1 revealed that the βL249Q mutant samples were ~10-fold less active than the wild type samples (Table 1). In all samples, the ATPase activity of both the mutant and the wild type enzymes was stimulated when *pmf* was dissipated by addition of uncouplers. The latter observation indicated that ATP hydrolysis both in the mutant and in the wild type EF_OF_1 was coupled to transmembrane proton pumping.

To check the coupling efficiency directly, we measured the ATP-driven proton pumping in proteoliposomes containing wild type or mutant EF_OF_1 with ACMA assay. As can be seen in Fig. 2, both samples demonstrated ATP-dependent proton transport. Noteworthy, DCCD (an inhibitor that specifically modifies F_O-portion and blocks the proton transport through it) completely abolished the ACMA quenching.

We also checked the effect of mutation on EF_OF_1 ATP synthesis activity in inverted *E. coli* membranes. As can be seen in Fig. 3, the rate of ATP synthesis by mutant membrane vesicles in response to succinate addition was very close to that of the wild type (0.2 ± 0.01 and 0.26 ± 0.04 U/mg of total membrane protein, correspondingly; given numbers are averages of 3 experiments).

The low ATPase activity that was strongly stimulated by sulfite in the mutant EF_1 (Fig. 1), and similar activities of the wild type and of

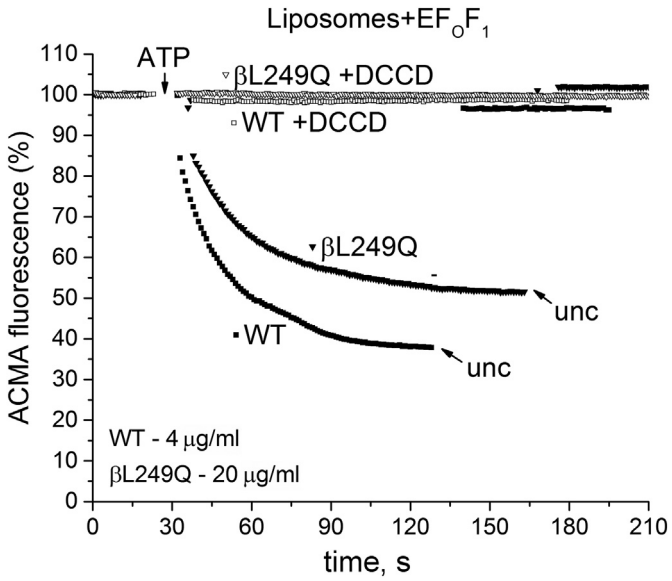

Fig. 2. ACMA quenching by proteoliposomes containing wild type or mutant βL249Q EF_OF_1. Proteoliposomes were mixed with the reaction buffer to the indicated concentration of EF_OF_1, then DCCD (to 100 μM) or the equal volume of EtOH was added. Samples were incubated at 37 °C for 20 min. Measurements were performed at room temperature. The proton pumping was started by addition of ATP to 500 μM. In DCCD(−) samples, the proton gradient on the membrane was dissipated by addition of valinomycin/nigericin mixture to 500 nM each (indicated as unc).

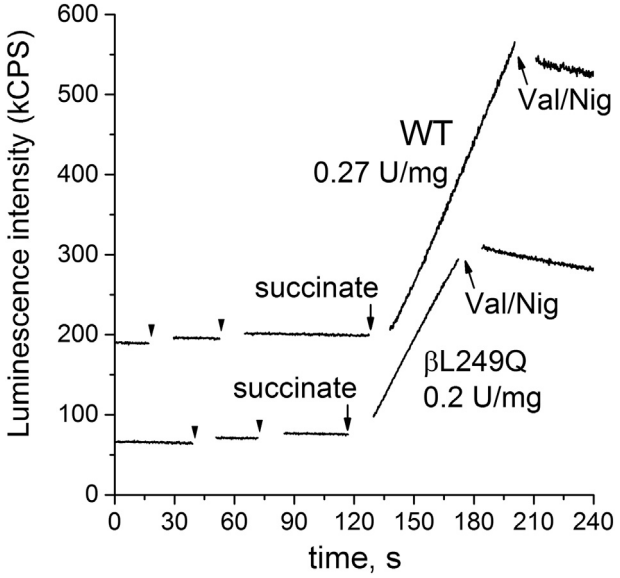

Fig. 3. ATP synthesis by inverted membrane vesicles of *Δunc E. coli* cells carrying wild type or mutant βL249Q pFV2. Short arrows indicate ATP additions to 100 nM which were used to calibrate the luciferase response. ATP synthesis was started by addition of sodium succinate to 4 mM and terminated by addition of valinomycin/nigericin mixture to 500 nM each. Total protein concentration in each sample was 54 μg/ml. See Materials and methods for experimental conditions.

βL249Q EF_OF_1 in ATP synthesis measurements suggested that the drop in ATP hydrolysis rate of the mutant enzyme could be a result of enhanced inhibition by MgADP. To verify this hypothesis, we measured the ATPase activity of wild type and mutant EF_OF_1 in membranes (native *E. coli* inverted vesicles and liposomes) by phenol red assay in the presence of sulfite. Since the energization of the membrane thermodynamically suppresses ATPase activity, all these experiments were performed under uncoupled conditions (samples contained 500 nM valinomycin + 500 nM nigericin) to cut off the *pmf* backpressure. We found that sulfite did not activate the hydrolysis of 1 mM ATP by wild type EF_OF_1 in inverted membrane vesicles (7,17 ± 1,1 U/mg with 5 mM sulfite, versus 7,08 ± 1,32 U/mg without sulfite). To confirm that the lack of sulfite activation was not due to the His-tag and Cys-to-Ala substitutions introduced in the EF_OF_1 in pFV2 plasmid, we have also measured the rate of ATP hydrolysis in inverted membranes from *E. coli* strain XL-1 Blue without pFV2 plasmid and with native ATP synthase operon in the genome. The ATPase activity measured by phenol red method with 1 mM ATP was 1.99 ± 0.22 U/mg without sulfite, and 1.82 ± 0.11 U/mg with 5 mM sulfite.

In proteoliposomes we observed a very modest, statistically insignificant sulfite stimulation of the wild type enzyme ATPase activity at 1 mM ATP (Fig. 4A). In contrast, the hydrolysis of 1 mM ATP by proteoliposomes containing βL249Q EF_OF_1 was stimulated by sulfite ~4-fold (Fig. 4B). When the hydrolysis was started by simultaneous addition of ATP to 750 μM and ADP to 250 μM, 5 mM sulfite activated both wild type and mutant enzymes, supporting the idea that sulfite effect is related to ADP-inhibition. Still, the mutant enzyme was stimulated stronger than the wild type EF_OF_1 (~9-fold and ~2-fold activation, respectively).

It was technically difficult to measure higher sulfite concentration effect with phenol red assay because sulfite has pH-buffering capacity, so we measured the sulfite dependence of ATPase activity of mutant and wild type EF_OF_1 in proteoliposomes by NADH assay (Fig. 5). Under these conditions, sulfite up to 5 mM did not affect the wild type enzyme but activated the mutant EF_OF_1 several fold. At 5 mM sulfite, the ATPase activity of βL249Q EF_OF_1 was 70% of the wild type activity, although in the absence of sulfite the activities differed by an order of

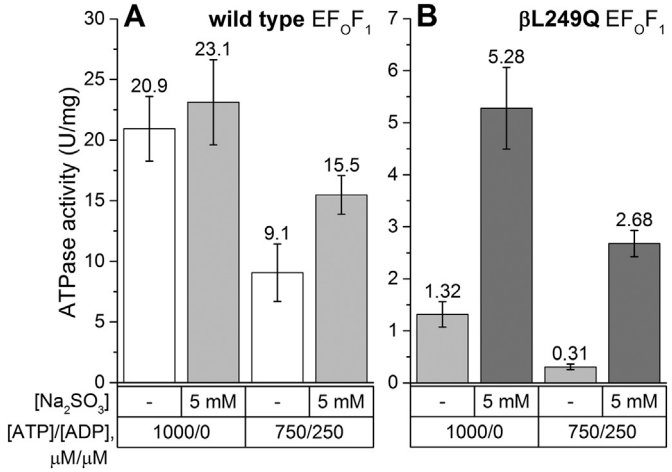

Fig. 4. ATP hydrolysis by uncoupled proteoliposomes containing (A) wild type or (B) βL249Q EF_OF_1 measured at 37 °C by phenol red assay (see Materials and methods for experimental conditions). Shown are average activities calculated from 3 traces each ± standard deviations. Hydrolysis was started by addition of ATP to 1 mM or ATP/ADP mix to 750 μM and 250 μM correspondingly. WT-EF_OF_1 concentrations were: 8 μg/ml at 1 mM ATP and 24 μg/ml when ADP was added. βL249Q-EF_OF_1 concentrations were: 58 μg/ml at 1 mM ATP and 124 μg/ml when ADP was added. Buffer contained the uncoupling mixture (valinomycin + nigericin, 500 nM each).

magnitude.

3.2. Inorganic phosphate stimulates ATP hydrolysis in βL249Q EF_OF_1

Besides weak ADP-inhibition, wild type EF_OF_1 has another feature distinguishing it from other ATP synthases characterized in literature. Many studies of ATP synthases from bacteria, chloroplasts, and mitochondria have shown that P_i counteracts ADP-inhibition and increases the ATPase activity of the enzyme (reviewed in [10]). However, Fischer et al. [13] have demonstrated that in *E. coli* F_OF_1 P_i significantly enhances the ADP-inhibition and suppresses the ATPase activity. In our experiments, P_i indeed inhibited the ATP hydrolysis by wild type EF_OF_1 (Figs. 6 and 7). Inverted membrane vesicles of *E. coli* carrying wild type pFV2 hydrolyzed 1 mM ATP about 2 times slower when 3 mM P_i was added to the reaction buffer (Fig. 6A). Purified wild type EF_OF_1 reconstituted into liposomes was also inhibited by P_i, although, when the proteoliposomes were not uncoupled, P_i caused only a moderate effect on the ATPase activity (Fig. 7A). However, under uncoupled conditions P_i inhibited the ATPase activity of wild type EF_OF_1 by half. The inhibitory effect of P_i on wild type EF_OF_1 was more pronounced when 250 μM ADP was added together with ATP, in agreement with earlier studies [13]. In that case, P_i inhibited the hydrolysis 3–4-fold, both in membrane particles and in proteoliposomes, and again the effect was stronger when the uncoupler was added. All these data are consistent with the hypothesis of mutually reinforcing inhibitory effects of P_i and MgADP on EF_OF_1.

In contrast, the ATP hydrolysis by inverted membrane vesicles containing mutant βL249Q EF_OF_1 was not inhibited by 3 mM P_i (Fig. 6B). In the experiments on proteoliposomes, P_i stimulated the ATPase activity of the mutant F_OF_1 (Fig. 7B).

The activation was more pronounced when either ADP or uncoupler were added. Maximal (2.6-fold) activation was observed when ADP and uncoupler were added together. In this case, the inhibitory effect of MgADP on ATPase activity was expected to be stronger, since *pmf* prevents the transition of the enzyme into ADP-inhibited state. We assumed that the stimulatory action of P_i on the mutant EF_OF_1 was likely caused by relieving ADP-inhibition. To verify this assumption, we examined the ATPase activities of liposomes containing wild type or βL249Q EF_OF_1 in ADP scavenging system by NADH assay (Fig. 8).

Compared to phenol red experiments, in ADP scavenging system 3 mM P_i inhibited the wild type enzyme by ~20% and slightly activated the mutant EF_OF_1. Such pattern is consistent with the hypothesis that the effect of P_i was related to ADP-inhibition. In these experiments, the presence of the uncoupler did not significantly influence the effect of P_i on either the wild type enzyme or on the mutant EF_OF_1. The highest tested concentration of P_i, 20 mM, inhibited both the wild type and the mutant EF_OF_1. Yet, under these conditions, the ATPase activity of the wild type enzyme was suppressed by 80%, whereas the mutant enzyme has lost only 20% of its activity.

4. Discussion

Non-competitive inhibition of the ATPase activity by MgADP is a universal feature found in all ATP synthases studied so far [10]. However, in EF_OF_1 it seems to be rather weak. We suggested that the degree of ADP-inhibition could be modulated by amino acid residues that are neither strictly conserved nor highly variable among enzymes from different organisms. The residue in position corresponding to β249 of EF_OF_1 is Gln in mitochondrial, chloroplastic and most bacterial enzymes, and Leu in many gammaproteobacteria (including *E. coli*) and betaproteobacteria. Previously it was demonstrated that replacement of Gln to Leu at this position significantly attenuates strong ADP-inhibition in the enzyme from thermophilic *Bacillus* sp. PS3 [15]. In this study, we had shown that mutation βL249Q in *E. coli* enzyme enhances ADP-inhibition. We had also observed no major effect of the mutation on ATP synthesis activity (Fig. 3) and on ATP-driven proton transport (Fig. 2), although in both experiments we cannot make precise quantitative estimates. The maximal ATP hydrolysis rate in the presence of sulfite (Figs. 1, 5A) that is known to relieve ADP-inhibition [18–21] was

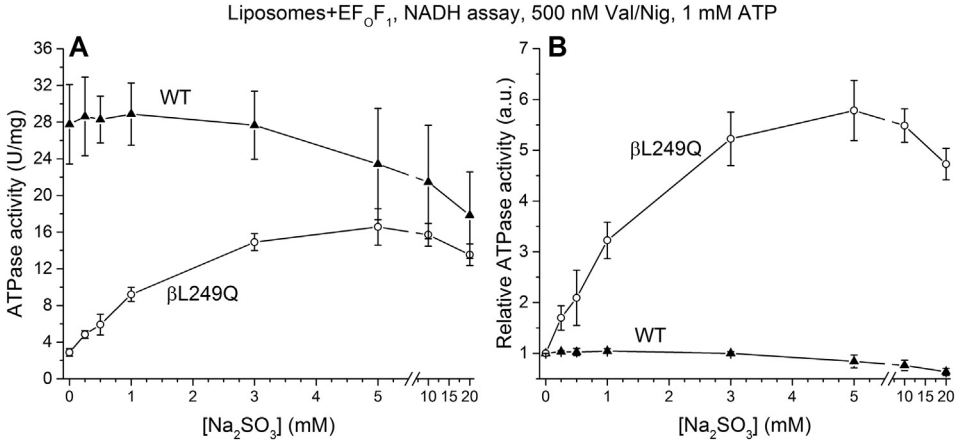

Fig. 5. ATP hydrolysis by uncoupled proteoliposomes containing wild type (black triangles) or βL249Q (open circles) EF_OF_1 measured at 37 °C by NADH assay at indicated sulfite concentrations. Shown are average activities calculated from 4 traces each ± standard deviations. (A) and (B) are the results of the same experiments. (A) ATPase activity is given in μmol ATP hydrolyzed in 1 min per 1 mg protein; (B) ATPase activity is normalized on the activity at zero sulfite concentration. Hydrolysis was started by addition of ATP to 1 mM. Buffer contained the uncoupling mixture (valinomycin + nigericin, 500 nM each).

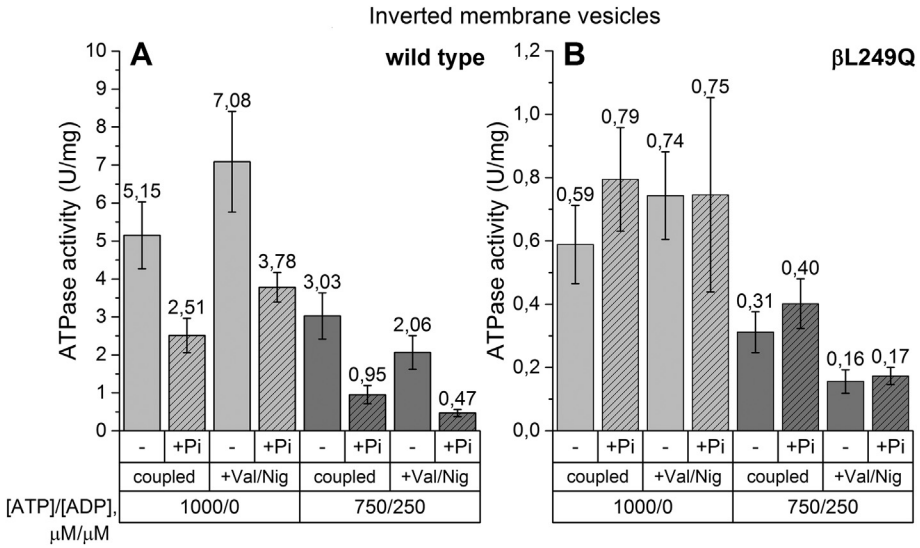

Fig. 6. ATP hydrolysis by inverted membrane vesicles of *Δunc E. coli* cells carrying (A) wild type or (B) mutant βL249Q pFV2 measured at 37 °C by phenol red assay. Shown are average activities calculated from 7 traces each ± standard deviations. Hydrolysis was started by addition of ATP to 1 mM or ATP/ADP mixture to 750 μM and 250 μM correspondingly. If indicated, buffer also contained 3 mM potassium phosphate (P_i), or uncoupler (valinomycin + nigericin, 500 nM each).

also similar in the wild type and in the mutant samples, suggesting that the mutation did not significantly impaired the catalytic 'core' of the enzyme. It is therefore likely that ADP-inhibition is not an inevitable side effect of the binding-change mechanism but a regulatory feature that can easily be affected by a point mutation, and is preserved by the evolution. In vivo strong ADP-inhibition might be important for prompt suppression of ATP hydrolysis by F_OF_1 to prevent the waste of ATP pool under conditions when the *pmf* generating enzymes activity decreases. On the other hand, a weaker ADP-inhibition in *E. coli* F_OF_1 (that, according to our results, is at least partially a consequence of Leu residue present in position β249) might be beneficial under low-oxygen conditions typical for *E. coli* natural habitat. Under such conditions, the primary role of F_OF_1 is not ATP synthesis but generation of *pmf* at the expense of ATP hydrolysis, and strong ADP-inhibition might be disadvantageous (see also [10] for a more detailed speculation on the physiological role of ADP-inhibition).

We have also found that mutation βL249Q changes the effect of P_i on the ATPase activity of *E. coli* F_OF_1. In the wild type enzyme P_i was shown to inhibit the activity and to enhance ADP-inhibition [13,14], in contrast to observations on F_OF_1 from other organisms, where P_i relieved ADP-inhibition [25–29]. According to the results in Figs. 6–8, P_i inhibited the ATPase activity of the wild type *E. coli* F_OF_1 in native membranes and in proteoliposomes.

It should be noted that the increase in the specific activity of F_OF_1 (estimated from measurements on inverted membranes and on proteoliposomes under uncoupled conditions with phenol red assay, Figs. 6 and 7) was approximately threefold for the wild type enzyme (7 U/mg → 21 U/mg) and twofold for the mutant (0.7 U/mg → 1.3 U/mg). Such relatively modest increase in specific activity might be due to partial activity loss during purification or to suboptimal lipid composition in proteoliposomes.

Both in native membranes and in proteoliposomes, the inhibitory effect of P_i for the wild type enzyme was stronger in the presence of ADP, in agreement with previous studies cited above. However, in the mutant βL249Q, P_i did not inhibit the ATPase activity (except 20 mM P_i, Fig. 8). On the contrary, in proteoliposomes the activity was stimulated by P_i. This effect was especially pronounced in the presence of ADP and uncouplers (> 2-fold stimulation, Fig. 7, B). It is probable that in the presence of *pmf* that is known to increase the affinity of the catalytic sites to P_i, traces of phosphate (tens of μM, plus P_i resulting from ATP hydrolysis during the reaction) present in the sample were already sufficient to prevent ADP-inhibition, so the increase in P_i

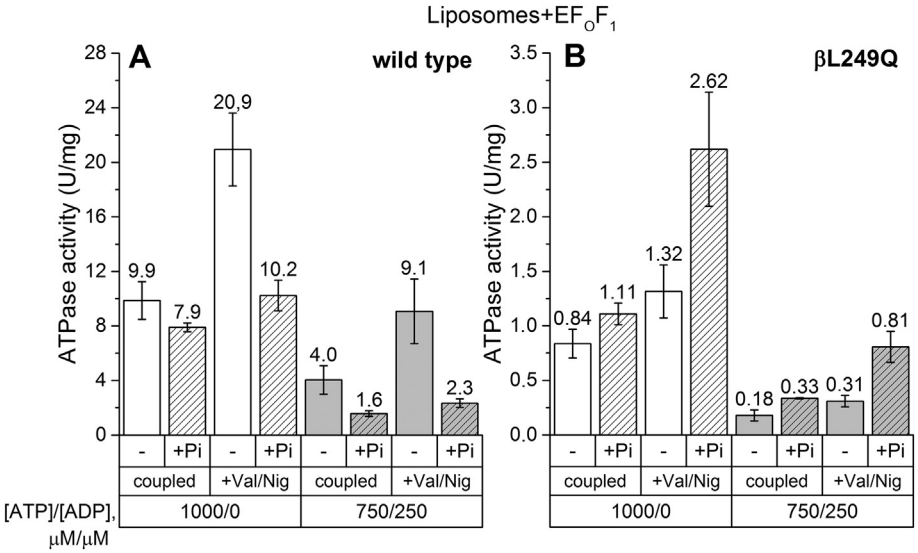

Fig. 7. ATP hydrolysis by proteoliposomes containing (A) wild type or (B) βL249Q EF_OF_1 measured at 37 °C by phenol red assay. Shown are average activities calculated from 3 traces each ± standard deviations. All reaction conditions were as in Fig. 6.

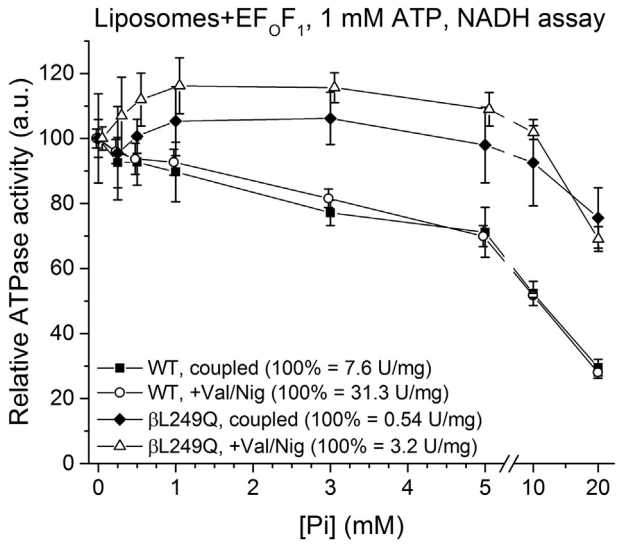

Fig. 8. ATP hydrolysis by proteoliposomes containing wild type or βL249Q EF_OF_1 measured at 37 °C by NADH assay at indicated P_i concentrations. The ATPase activity is normalized to the activity without P_i addition. The absolute activities corresponding to 100% are indicated for each curve. Dots are average activities calculated from 4 traces each ± standard deviations. Hydrolysis was started by addition of ATP to 1 mM. The measurements were performed under coupling conditions or in the presence of valinomycin/nigericin, 500 nM each. Buffer contained 2.5 mM $MgCl_2$.

concentration to 3 mM had no major effect.

It should be noted that the patterns of ATPase activity changes induced by ADP, P_i, and uncouplers were somewhat different when measured in the inverted membranes (Fig. 6) and in proteoliposomes (Fig. 7). Namely, i) uncouplers stimulated ATP hydrolysis stronger in proteoliposomes than in inverted membranes; ii) under uncoupled conditions, P_i stimulated the activity of the mutant in proteoliposomes, but had no statistically significant effect in inverted membranes (both at 1 mM ATP and at 0.75/0.25 mM ATP/ADP); iii) under uncoupled conditions, the inhibition of the wild type enzyme ATPase activity in response to ADP concentration increase was stronger in inverted membranes than in proteoliposomes. The difference in the stimulation by uncouplers can be explained by lower passive H^+-conductance of proteoliposomes membranes in comparison to that of native *E. coli* membranes of inverted vesicles. Without uncouplers the ATPase activity in membrane vesicles (both native or artificial) is expected to be limited by the rate of passive H^+ leak, and should be lower in vesicles with less H^+-conductance. The causes for differences ii) and iii) are less evident. One may speculate that a possible cause was a different nucleotide occupancy of the F_OF_1 non-catalytic sites that was not monitored in our experiments. In inverted membranes, the non-catalytic sites might retain nucleotides (ATP and ADP), while in proteoliposomes the enzyme might initially have no nucleotides bound, because they could have got washed off during F_OF_1 purification procedure in the presence of detergents. The occupancy of the non-catalytic sites by ATP and ADP is known to modulate ADP-inhibition [10]. However, other explanations for the differences observed are possible, and further experiments are necessary to clarify this issue.

We had also found that sulfite stimulated ATP hydrolysis in the mutant enzyme more efficiently than in the wild type F_OF_1. According to the studies on chloroplast F_OF_1 [18,21], P_i and sulfite compete for binding to the catalytic sites, and the activation of ATP hydrolysis by both anions is likely explained by attenuation of ADP-inhibition. Earlier studies on EF_1 revealed that 7.5 mM sulfite facilitates the release of the inhibitory ADP from the catalytic sites of the enzyme [12] and that 40 mM sulfite stimulates the ATPase activity of *E. coli* $\alpha_3\beta_3\gamma\delta$-complex approximately fourfold [30].

In the presence of the ATP-regenerating system we observed no activation by 0.25–8 mM sulfite in wild type *E. coli* F_OF_1 and F_1, while the mutant enzymes were strongly activated by sulfite (Figs. 1 and 5). In phenol red assay experiments the ATPase activity of βL249Q EF_OF_1 was also markedly stimulated by 5 mM sulfite, and the stimulation was significantly enhanced in the presence of 250 μM ADP (~4-fold and ~8-fold, respectively). On the contrary, the wild type EF_OF_1 was stimulated by sulfite only when ADP was added together with ATP. Taken together, the results of our experiments with sulfite indicate that the activation of ATP hydrolysis was likely caused by attenuation of ADP-inhibition, and that mutation βL249Q enhanced ADP-inhibition in EF_OF_1.

According to the structure obtained by X-ray crystallography for EF_1 [31], the residue β249 is located near the catalytic site in the cleft between α and β subunits, approximately 1.2 nm from the phosphate-binding site. It is possible that the βL249Q mutation altered the position of βArg246 sidechain that is intercalated between the P_i-binding site (occupied by sulfate in the structure) and residue β249. The guanidinium group of βArg246 interacts with two oxygens of P_i, and if the mutation resulted in disruption of this interaction, it could have a significant effect on the P_i binding affinity at the catalytic site. However, it cannot be excluded that the influence of the mutation is mediated by overall change in the α/β interface structure near the catalytic site. Detailed clarification of the molecular mechanism of ADP-inhibition requires further experimental studies. Several mutations, including those of residues very distant from the catalytic sites, were shown to modulate ADP-inhibition in ATP synthase. Substitution of four positively charged residues at the N-terminus of subunit γ (Lys8, Arg9, Arg10, and Arg12) by glutamines in F_1 complex from thermoalkaliphilic bacterium *Caldalkalibacillus thermarum* (also known as *Bacillus* sp. TA2.A1) resulted in a 35-fold increase in the rate of ATP hydrolysis, likely because of attenuation of ADP-inhibition [32]. Mutation γM23K in ATP synthase from purple bacterium *Rhodobacter capsulatus*, on the contrary, enhanced ADP-inhibition [33]. In both cases, the effect was hardly caused by direct influence of the substitutions in subunit γ on the catalytic sites. An alternative interpretation was that mutations altered the stability of subunit γ angular position corresponding to F_1 conformation that is prone to transition to the ADP-inhibited state.

Mutation βT165S in the P-loop of *Bacillus* sp. PS3 enzyme was shown to prevent the formation of the ADP-inhibited state, and led to an increase in the ATPase activity [34]. The same effect was observed upon mutation of the homologous residue in *E. coli* enzyme [35] and in F_OF_1 from *Saccharomyces cerevisiae* mitochondria [36]. In this case, direct effect on the P_i binding in the catalytic site seems probable. However, unlike the residue at position corresponding to *E. coli* β249 studied in our work, threonine at position corresponding to βT165S of *Bacillus* sp. PS3 enzyme is absolutely conserved in all ATP synthases. It is probable that, besides modulation of the ADP-inhibition, this residue is responsible for other physiologically important characteristics of the enzyme and is therefore preserved by evolution.

Supplementary data to this article can be found online at https://doi.org/10.1016/j.bbabio.2018.12.003.

Transparency document

The Transparency document associated with this article can be found, in online version.

Acknowledgements

The authors would like to thank Mr. Evgenii Borisov for help with EF_1 preparation and experiments, and the anonymous reviewers of the manuscript for valuable comments and suggestions.

Funding

This work was supported by the Russian Science Foundation research project no. 14-14-00128.

Authors' contributions

Anna Lapashina: Investigation, Validation, Methodology, Formal Analysis, Writing – Original Draft. **Anastasia Prikhodko:** Investigation, Formal Analysis. **Tatiana Shugaeva:** Investigation, Validation, Formal Analysis, Software. **Boris Feniouk:** Conceptualization, Methodology, Formal Analysis, Writing – Original Draft, Supervision, Project Administration, Funding Acquisition.

References

[1] W. Jiang, J. Hermolin, R.H. Fillingame, The preferred stoichiometry of c subunits in the rotary motor sector of *Escherichia coli* ATP synthase is 10, Proc. Natl. Acad. Sci. U. S. A. 98 (2001) 4966–4971, https://doi.org/10.1073/pnas.081424898.

[2] B. Ballhausen, K. Altendorf, G. Deckers-Hebestreit, Constant c10 ring stoichiometry in the *Escherichia coli* ATP synthase analyzed by Cross-linking, J. Bacteriol. 191 (2009) 2400–2404, https://doi.org/10.1128/JB.01390-08.

[3] A.G. Stewart, E.M. Laming, M. Sobti, D. Stock, Rotary ATPases—dynamic molecular machines, Curr. Opin. Struct. Biol. 25 (2014) 40–48, https://doi.org/10.1016/j.sbi.2013.11.013.

[4] R. Watanabe, Rotary catalysis of FoF1-ATP synthase, Biophysics 9 (2013) 51–56, https://doi.org/10.2142/biophysics.9.51.

[5] W. Junge, N. Nelson, ATP synthase, Annu. Rev. Biochem. 84 (2015) 631–657, https://doi.org/10.1146/annurev-biochem-060614-034124.

[6] B.A. Feniouk, M. Yoshida, Regulatory mechanisms of proton-translocating F(O)F(1)-ATP synthase, Results Probl. Cell Differ. 45 (2008) 279–308, https://doi.org/10.1007/400_2007_043.

[7] H. Sielaff, T.M. Duncan, M. Börsch, The regulatory subunit ε in *Escherichia coli* FOF1-ATP synthase, Biochim. Biophys. Acta Bioenerg. 1859 (2018) 775–788, https://doi.org/10.1016/j.bbabio.2018.06.013.

[8] T. Hisabori, H. Konno, H. Ichimura, H. Strotmann, D. Bald, Molecular devices of chloroplast F(1)-ATP synthase for the regulation, Biochim. Biophys. Acta 1555 (2002) 140–146 https://www.ncbi.nlm.nih.gov/pubmed/12206906.

[9] M. Campanella, N. Parker, C.H. Tan, A.M. Hall, M.R. Duchen, IF(1): setting the pace of the F(1)F(o)-ATP synthase, Trends Biochem. Sci. 34 (2009) 343–350, https://doi.org/10.1016/j.tibs.2009.03.006.

[10] A.S. Lapashina, B.A. Feniouk, ADP-inhibition of H+-FOF1-ATP synthase, Biochem. Mosc. (10) (2018) 1141–1160, https://doi.org/10.1134/S0006297918100012.

[11] A.E. Senior, R.S. Lee, M.K. al-Shawi, J. Weber, Catalytic properties of *Escherichia coli* F1-ATPase depleted of endogenous nucleotides, Arch. Biochem. Biophys. 297 (1992) 340–344 https://www.ncbi.nlm.nih.gov/pubmed/1386723.

[12] D.J. Hyndman, Y.M. Milgrom, E.A. Bramhall, R.L. Cross, Nucleotide-binding sites on *Escherichia coli* F1-ATPase. Specificity of noncatalytic sites and inhibition at catalytic sites by MgADP, J. Biol. Chem. 269 (1994) 28871–28877 https://www.ncbi.nlm.nih.gov/pubmed/7961847.

[13] S. Fischer, P. Graber, P. Turina, The activity of the ATP synthase from *Escherichia coli* is regulated by the transmembrane proton motive force, J. Biol. Chem. 275 (2000) 30157–30162, https://doi.org/10.1074/jbc.M004135200.

[14] M. D'Alessandro, P. Turina, B.A. Melandri, Intrinsic uncoupling in the ATP synthase of *Escherichia coli*, Biochim. Biophys. Acta 1777 (2008) 1518–1527, https://doi.org/10.1016/j.bbabio.2008.09.011.

[15] B.A. Feniouk, C. Wakabayashi, T. Suzuki, M. Yoshida, A point mutation, betaGln259Leu, relieves MgADP inhibition in Bacillus PS3 ATP synthase, Biochim. Biophys. Acta Bioenerg. 1817 (2012) S13, https://doi.org/10.1016/j.bbabio.2012.06.045.

[16] R.R. Ishmukhametov, M.A. Galkin, S.B. Vik, Ultrafast purification and reconstitution of His-tagged cysteine-less *Escherichia coli* F1Fo ATP synthase, Biochim. Biophys. Acta 1706 (2005) 110–116, https://doi.org/10.1016/j.bbabio.2004.09.012.

[17] K.A. Datsenko, B.L. Wanner, One-step inactivation of chromosomal genes in *Escherichia coli* K-12 using PCR products, Proc. Natl. Acad. Sci. U. S. A. 97 (2000) 6640–6645, https://doi.org/10.1073/pnas.120163297.

[18] Z.Y. Du, P.D. Boyer, On the mechanism of sulfite activation of chloroplast thylakoid ATPase and the relation of ADP tightly bound at a catalytic site to the binding change mechanism, Biochemistry 29 (1990) 402–407 https://www.ncbi.nlm.nih.gov/pubmed/2137348.

[19] P. Cappellini, P. Turina, V. Fregni, B.A. Melandri, Sulfite stimulates the ATP hydrolysis activity of but not proton translocation by the ATP synthase of *Rhodobacter capsulatus* and interferes with its activation by delta muH+, Eur. J. Biochem. 248 (1997) 496–506 https://www.ncbi.nlm.nih.gov/pubmed/9346308.

[20] F. Pacheco-Moisés, J.J. García, J.S. Rodríguez-Zavala, R. Moreno-Sánchez, Sulfite and membrane energization induce two different active states of the *Paracoccus denitrificans* F0F1-ATPase, Eur. J. Biochem. 267 (2000) 993–1000 https://www.ncbi.nlm.nih.gov/pubmed/10672007.

[21] R.H. Bakels, J.E. Van Wielink, K. Krab, H.S. Van Walraven, The effect of sulfite on the ATP hydrolysis and synthesis activities in chloroplasts and cyanobacterial membrane vesicles can be explained by competition with phosphate, Arch. Biochem. Biophys. 332 (1996) 170–174, https://doi.org/10.1006/abbi.1996.0329.

[22] P.C. Sternweis, J.B. Smith, Characterization of the inhibitory (epsilon) subunit of the proton-translocating adenosine triphosphatase from *Escherichia coli*, Biochemistry 19 (1980) 526–531 https://www.ncbi.nlm.nih.gov/pubmed/6444514.

[23] S.D. Dunn, The isolated gamma subunit of *Escherichia coli* F1 ATPase binds the epsilon subunit, J. Biol. Chem. 257 (1982) 7354–7359 https://www.ncbi.nlm.nih.gov/pubmed/6211441.

[24] M.K. Al-Shawi, C.J. Ketchum, R.K. Nakamoto, Energy coupling, turnover, and stability of the F0F1 ATP synthase are dependent on the energy of interaction between gamma and beta subunits, J. Biol. Chem. 272 (1997) 2300–2306 https://www.ncbi.nlm.nih.gov/pubmed/8999937.

[25] B.A. Feniouk, T. Suzuki, M. Yoshida, Regulatory interplay between proton motive force, ADP, phosphate, and subunit ε in bacterial ATP synthase, J. Biol. Chem. 282 (2007) 764–772, https://doi.org/10.1074/jbc.M606321200.

[26] T.V. Zharova, A.D. Vinogradov, Energy-dependent transformation of F0.F1-ATPase in *Paracoccus denitrificans* plasma membranes, J. Biol. Chem. 279 (2004) 12319–12324, https://doi.org/10.1074/jbc.M311397200.

[27] N. Mitome, S. Ono, T. Suzuki, K. Shimabukuro, E. Muneyuki, M. Yoshida, The presence of phosphate at a catalytic site suppresses the formation of the MgADP-inhibited form of F(1)-ATPase, Eur. J. Biochem. 269 (2002) 53–60 https://www.ncbi.nlm.nih.gov/pubmed/11784298.

[28] P. Turina, B. Rumberg, B.A. Melandri, P. Gräber, Activation of the H (+)-ATP synthase in the photosynthetic bacterium *Rhodobacter capsulatus*, J. Biol. Chem. 267 (1992) 11057–11063 http://www.jbc.org/content/267/16/11057.short.

[29] C. Carmeli, Y. Lifshitz, Effects of P 1 and ADP on ATPase activity in chloroplasts, Biochim. Biophys. Acta 267 (1972) 86–95 https://www.ncbi.nlm.nih.gov/pubmed/4259760.

[30] S.D. Dunn, V.D. Zadorozny, R.G. Tozer, L.E. Orr, Epsilon subunit of *Escherichia coli* F1-ATPase: effects on affinity for aurovertin and inhibition of product release in unisite ATP hydrolysis, Biochemistry 26 (1987) 4488–4493 https://www.ncbi.nlm.nih.gov/pubmed/2889464.

[31] G. Cingolani, T.M. Duncan, Structure of the ATP synthase catalytic complex (F(1)) from *Escherichia coli* in an autoinhibited conformation, Nat. Struct. Mol. Biol. 18 (2011) 701–707, https://doi.org/10.1038/nsmb.2058.

[32] A. Stocker, S. Keis, J. Vonck, G.M. Cook, P. Dimroth, The structural basis for unidirectional rotation of thermoalkaliphilic F1-ATPase, Structure 15 (2007) 904–914, https://doi.org/10.1016/j.str.2007.06.009.

[33] B.A. Feniouk, A. Rebecchi, D. Giovannini, S. Anefors, A.Y. Mulkidjanian, W. Junge, P. Turina, B.A. Melandri, Met23Lys mutation in subunit gamma of F(O)F(1)-ATP synthase from *Rhodobacter capsulatus* impairs the activation of ATP hydrolysis by protonmotive force, Biochim. Biophys. Acta 1767 (2007) 1319–1330, https://doi.org/10.1016/j.bbabio.2007.07.009.

[34] J.-M. Jault, C. Dou, N.B. Grodsky, T. Matsui, M. Yoshida, W.S. Allison, The α3β3γ subcomplex of the F1-ATPase from the thermophilic *Bacillus* PS3 with the βT165S substitution does not entrap inhibitory MgADP in a catalytic site during turnover, J. Biol. Chem. 271 (1996) 28818–28824, https://doi.org/10.1074/jbc.271.46.28818.

[35] H. Omote, M. Maeda, M. Futai, Effects of mutations of conserved Lys-155 and Thr-156 residues in the phosphate-binding glycine-rich sequence of the F1-ATPase beta subunit of *Escherichia coli*, J. Biol. Chem. 267 (1992) 20571–20576 https://www.ncbi.nlm.nih.gov/pubmed/1400377.

[36] D.M. Mueller, A mutation altering the kinetic responses of the yeast mitochondrial F1-ATPase, J. Biol. Chem. 264 (1989) 16552–16556 https://www.ncbi.nlm.nih.gov/pubmed/2528546.